Submitted to Cold Regions Science and Technology, December 198

A MULTIAXIAL DIFFERENTIAL FLOW LAW FOR POLYCRYSTALLINE ICE

S. Shyam Sunder and Mao S. Wu
Massachusetts Institute of Technology, Department of Civil Engineering, Room 1-274, Cambridge, MA 02139

---

1. INTRODUCTION

Boundary value problems in applied ice mechanics involving multiaxial states of stress and complex loading histories, such as those encountered during ice-structure interaction, are increasingly being solved using numerical models including the finite element method (Jordaan, 1986). Constitutive models are required to characterize the ice deformation by viscoelastic flow in numerical simulations.

In problems where only "steady state" flow is of interest, an elastic - power law creep model of ice (sometimes without the elastic component) is adequate. The most widely used model of steady state or viscous flow of polycrystalline ice is Glen's power law. The multiaxial generalization of the differential model follows from conventional elasticity theory and from the rate theory of flow. The latter is based on normality of the viscous deformation-rate to a scalar valued flow potential expressed in terms of an equivalent stress measure. Palmer (1967) has derived the multiaxial law for incompressible flow of isotropic ice, while Shyam Sunder, Ganguly and Ting (1987) have presented an orthotropic model of incompressible flow.

Both the elastic and "transient" flow behavior of ice, however, are of great importance in a broad range of ice mechanics problems (Gold, 1977, Sinha et al., 1987). The most widely used flow law for ice under uniaxial loading is the creep compliance function proposed by Sinha (1978, 1979). This formulation postulates that grain boundary sliding governs transient deformation, and that the compliance function is linearly dependent on stress and nonlinearly dependent on time. For conditions other than constant stress creep, monotonically increasing stress in particular, Sinha (1983) has applied the nonlinear compliance function in conjunction with a convolution integral to predict the mechanical behavior. This integral formulation assumes a particular generalization of Boltzmann's superposition principle for transient deformations.

Le Gac and Duval (1980) have proposed multiaxial constitutive relations for the inelastic deformation of polycrystalline ice which account for the phenomena of isotropic and kinematic hardening. Considering deformation mechanisms in ice, Ashby and Duval (1985) have subsequently developed a kinematic hardening model based on a two-bar truss analogy. They have used the model to identify certain dimensionless variables from which a single master curve can be developed for the creep of polycrystalline ice. The appropriateness of the variables has been demonstrated using the comprehensive experimental data of Jacka (1984) for dense isotropic polycrystals with a mean grain size of 1.7 mm. The predictive capability of their model, however, has not been explicitly tested against this data set.

This paper presents a differential flow model for the deformation of polycrystalline ice which (i) accounts for both isotropic and kinematic hardening, and (ii) satisfies the dimensional requirements identified by Ashby and Duval (1985). Flow (or creep) is modeled in terms of two nonlinear deformation-rate mechanisms: the first mechanism governs the transient deformation-rate (creep) which decays to zero as both an elastic back stress and a drag stress measure increase asymptotically; the second mechanism, which is modeled in terms of the well-known power law, governs the viscous deformation-rate. The evolution of the back or rest stress contributes to kinematic hardening, while that of the drag stress contributes to isotropic hardening.

In general, numerical integration of the governing equations is necessary for predicting the model response under arbitrary loading histories since both isotropic and kinematic hardening are history dependent phenomena. However, closed form analytical solutions are available for the creep compliance function and the recovery response if only kinematic hardening is considered. When both types of hardening are included, the differential model follows creep data on ice quite well, specifically those of Jacka (1984). Predictions of the ratio of transient (delayed elastic) strain to total strain agree qualitatively with Sinha's (1979) model if grain size effects are taken into account.

The multiaxial generalization of the differential model follows from conventional elasticity theory and from the rate theory of flow. This eliminates the need for an integral formulation under variable loading histories or multiaxial loading and for generalizing the superposition assumption for nonlinearly viscoelastic materials. Equations are derived for an orthotropic model of incompressible flow and for estimating model parameters from uniaxial experimental data.

2. UNIAXIAL DIFFERENTIAL MODEL

Physical Basis of Deformation Model.-- There is general agreement, based on theoretical and experimental work, that at least two thermally activated deformation systems, a soft system and a hard system, are present during the flow of fresh-water polycrystalline ice (Sinha, 1979, Ashby and Duval, 1985.) They may be either grain boundary sliding (with diffusional accommodation) and basal slip or basal slip and slip on a non-basal plane. A combination of these processes could be present as well.

Initially, the solid resists the applied stresses in an elastic manner and then flow begins on the soft and hard systems. However, flow, particularly on the easy soft system, causes the build-up of internal elastic stresses. This may occur as a result of grain boundary sliding next to grains poorly aligned for deformation or dislocation pile-ups at the boundaries of such grains. Dislocation pile-ups at grain boundaries have been observed in ice through scanning electron microscopy (Sinha, 1987.) The internal elastic stresses, termed back or rest stresses, resist flow. In addition, internal drag stresses which resist dislocation fluxes are generated in annealed materials undergoing flow. The increase in drag stresses are the outcome of creep resistant substructures, i.e., subgrains and cells, formed by grain boundary sliding or dislocation movement and of dilocation entanglement, dipole formation and kink band formation during slip (particularly on the basal plane.)

A detailed understanding of evolving structural and stress states on the deformation of polycrystalline materials is unavailable at the present time. For example, only recently has an attempt been made to model the primary creep process resulting from sub-cell formation using sub-cell size and misorientation as state variables (Derby and Ashby, 1987.) However, it is well known that an increasing drag stress contributes to isotropic hardening, while an increasing rest stress contributes to kinematic hardening. In isotropic hardening, material properties are independent of the direction of straining. On the other hand, kinematic hardening induces directionally dependent material properties, referred to as deformation or stress-induced anisotropy. The Baushinger effect in metals is an example of kinematic hardening.

In this paper, the deformations resulting from the interactions between the soft and hard systems are decomposed into two components; a transient flow component and a steady flow component. Steady state flow, representing a balance between work-hardening and recovery, is associated with viscous (irrecoverable) strains. Isotropic and kinematic hardening phenomena are active during transient flow and give rise to elastic strains. These strains are recoverable on unloading since equilibrium requires the internal elastic back stress to reduce to zero. The time-dependent elastic strains defining transient deformation represent the phenomenon of delayed elasticity or anelasticity.

Mathematical Formulation.-- The governing equation for the model under uniaxial conditions is obtained by expressing the total strain rate as a sum of its components, i.e.:

$$\dot{\varepsilon} = \dot{\varepsilon}_e + \dot{\varepsilon}_t + \dot{\varepsilon}_v \qquad (1)$$

where the three terms on the right hand side, representing instantaneous elasticity, transient flow and steady state or viscous flow are described in what follows.

The instantaneous elastic strain, ε_e, is related to the stress, σ, through the Young's modulus, E, of polycrystalline ice; this relationship may be expressed in rate form as:

$$\dot{\varepsilon}_e = \dot{\sigma}/E \tag{2}$$

Several investigators (see, e.g., Gold, 1977) have shown using high-frequency sonic methods that the Young's modulus of polycrystalline fresh-water ice varies in the range of 9-11 GPa, with negligible temperature dependence between -5°C and -45°C.

The viscous strain, ε_v, which is associated with secondary creep or steady flow conditions, follows the well known Norton type power law of Glen (1955), i.e.,

$$\sigma = V \dot{\varepsilon}_v^{1/N} \tag{3}$$

where N is the power law index and V is a temperature dependent constant characterized by an Arrhenius activation energy law:

$$V = V_o \exp(Q/NRT) \tag{4}$$

T is the temperature in Kelvin, V_o is a temperature independent constant, Q is the activation energy, and R is the universal gas constant equal to 8.32 J mol^{-1} K^{-1}. The activation energy for steady flow of columnar-grained polycrystalline ice has been experimentally determined by Gold (1973) to be 65 KJ mol^{-1} for temperatures in the range of -5°C to -40°C. While the activation energy for pure single crystals does not change with temperature up to -0.2°C, Gold (1983) suggests that Q varies at the higher temperatures for polycrystalline ice and that at temperatures greater than -5°C it is probably closer to 100 KJ mol^{-1}. Similar trends have been observed by Barnes et al. (1971.)

The transient strain rate $\dot{\varepsilon}_t$ is taken to follow a Norton type power law driven by a reduced stress measure, σ_r, i.e.,

$$\dot{\varepsilon}_t = (\sigma_r/V)^N = \left[\frac{\sigma - R}{BV}\right]^N \tag{5}$$

where the variable R represents the back stress and B is a non-dimensional drag stress. Implicit in the formulation of Eq. (5) are the assumptions that: (i) the exponent N is the same as that for steady flow in Eq. (2), and (ii) the temperature dependence of the transient deformation-rate, represented by the parameter V, is given by an Arrhenius law with an activation energy equal to that for steady flow. For columnar-grained polycrystalline (fresh-water) ice the former assumption can be deduced from the numerical values for parameters in Sinha's (1978) time-hardening model, and for dense isotropic polycrystals from the strain-hardening model of Ashby and Duval (1985). Sinha (1978) has also shown that the activation energy for transient flow is equal to 67 KJ mol^{-1}, which agrees well with Gold's (1973) data for steady flow in the same type of ice.

Evolution equations must be specified for R and B which are history-dependent variables representing transient flow. Since the transient strains are elastic in nature, the time rates of change of the back and drag stresses are linearly proportional to the transient strain rate. The following equations are postulated to descibe the evolution of R and B:

$$\dot{R} = AE\,\dot{\varepsilon}_t \tag{6}$$

$$\dot{B} = H\,|\dot{\varepsilon}_t|\,\mathrm{sgn}\left[\frac{d|\varepsilon_t|}{dt}\right] \tag{7}$$

The initial value of R is zero for an annealed material or for a material that has recovered from prior loading. On the other hand the initial value of B, i.e., B_o, may represent the annealed state of the material or some level of initial hardening introduced by pre-straining. Both A and H are temperature independent and dimensionless variables.

Under creep loading R will asymptotically increase to a value equal to the applied stress, at which point transient flow will cease. In the case of constant strain rate loading, R approaches the steady state stress asymptotically. The maximum value of transient strain in both these cases is given by $\varepsilon_{t,max}=\sigma/AE$ when R is zero initially. A value of A less than one suggests that this magnitude is greater than the instantaneous elastic strain. For the same loading conditions, the drag stress reaches a maximum value equal to $B_o+H\varepsilon_{t,max}$. This constraint on the maximum value of B states that the isotropic resistance to transient flow is not unbounded; if it is unbounded and approaches infinity, the material will lose its ability to undergo further flow.

Under reversed or cyclic loading R will reverse or switch back and forth between positive and negative values, i.e., the physical processes associated with kinematic hardening can locally relax or move back and forth, thus preventing a continual build-up which would lead to considerable hardening. The signum function is used in Eq. (7) to ensure that B has the same effect on material behavior under both compressive and tensile loadings. For instance, it can be inferred from Eq. (7) that $\dot{B} > 0$ during both tensile and compressive creep tests, while it is negative during unloading in both types of tests. The decrease in drag stress during unloading indicates a decreasing resistance to grain boundary sliding and dislocation fluxes. This may arise from a spatial bias in the distribution of defects generated by isotropic hardening which favors regions of high back stress concentration.

Equations (1)-(7) define the governing differential equations for the uniaxial model. For creep loading, the solutions of Eqs. (1)-(4) are trivial. However, Eqs. (5)-(7) are coupled and numerical integration is necessary to compute the transient strains if both isotropic and kinematic hardening are present. If isotropic hardening is absent, i.e., B is a constant, analytical solutions can be obtained as shown in a subsequent section. For a general or variable loading history, the governing equations are all coupled and numerical integration is required.

Model Formulation in Dimensionless Variables.-- For the special cases of constant stress and constant strain rate loading, Ashby and Duval (1985) have suggested that unique relationships exist between certain dimensionless variables. Such relationships are predicted by the proposed model as shown below.

For creep of polycrystalline ice at constant applied stress, Ashby and Duval (1985) have considered the following dimensionless variables for strain, strain rate, time, and the back stress:

$$\tilde{\varepsilon} = \varepsilon E/\sigma \tag{8}$$

$$\tilde{\dot{\varepsilon}} = \dot{\varepsilon}/\dot{\varepsilon}_v \tag{9}$$

$$\tilde{t} = t\dot{\varepsilon}_v E/\sigma \tag{10}$$

$$\tilde{R} = R/\sigma \tag{11}$$

Substituting Eqs. (8)-(11) in Eqs. (2), (3) and (5) yields:

$$\tilde{\varepsilon}_e = 1 \tag{12}$$

$$\tilde{\varepsilon}_v = \tilde{t} \tag{13}$$

and

$$\tilde{\dot{\varepsilon}}_v = 1 \tag{14}$$

$$R + B\tilde{\dot{\varepsilon}}_t^{\,1/N} = 1 \tag{15}$$

In order that Eq. (7) also reduces to a dimensionless form, the hardening parameter H is defined as $\tilde{H}E/\sigma$. The dimensionless evolution equations can then be expressed as:

$$\dot{\tilde{R}} = A\tilde{\dot{\varepsilon}}_t \tag{16}$$

$$\frac{dB}{d\tilde{t}} = \tilde{H}\,|\tilde{\dot{\varepsilon}}_t|\ \operatorname{sgn}\left[\frac{d\,|\varepsilon_t|}{d\,\tilde{t}}\right] \tag{17}$$

In the above equations the differentiation is with respect to dimensionless time. Equations (12)-(17) show that the model predicts a unique relationship between the dimensionless variables and is independent of applied stress level and temperature.

Under constant strain rate loading the model predicts that a unique relationship exists between dimensionless stress $\tilde{\sigma}$ and dimensionless time $\tilde{t}$, independent of the applied strain rate $\dot{\varepsilon}_a$ and temperature. Consider the following dimensionless variables for stresses, time, and strains, as suggested by Ashby and Duval (1985):

$$\tilde{\sigma} = \frac{\sigma}{\sigma_{min}} ; \qquad \tilde{R} = \frac{R}{\sigma_{min}} \tag{18}$$

$$\tilde{t} = \frac{t\dot{\varepsilon}_a E}{\sigma_{min}} \tag{19}$$

$$\tilde{\varepsilon}_e = \frac{\varepsilon_e E}{\sigma} ; \qquad \tilde{\varepsilon}_v = \frac{\varepsilon_v E}{\sigma} ; \qquad \tilde{\varepsilon}_t = \frac{\varepsilon_t E}{\sigma} \tag{20}$$

where σ_{min} is the stress corresponding to the minimum creep rate given by Glen's power law, Eq. (3):

$$\sigma_{min} = V \, \dot{\varepsilon}_a^{\,1/N} \tag{21}$$

Substituting Eqs. (18)-(20) in Eqs. (2), (3), (5)-(7) yields:

$$\dot{\tilde{\varepsilon}}_e = \frac{\dot{\tilde{\sigma}}}{\tilde{\sigma}} (1 - \tilde{\varepsilon}_e) \tag{22}$$

$$\dot{\tilde{\varepsilon}}_v = \frac{1}{\tilde{\sigma}} [\tilde{\sigma}^N - \tilde{\varepsilon}_v \, \dot{\tilde{\sigma}}] \tag{23}$$

$$\dot{\tilde{\varepsilon}}_t = \frac{1}{\tilde{\sigma}} \left[\frac{\tilde{\sigma} - \tilde{R}}{B}\right]^N - \frac{\tilde{\varepsilon}_t}{\tilde{\sigma}} \, \dot{\tilde{\sigma}} \tag{24}$$

$$\tilde{R} = A \frac{d}{d\tilde{t}} [\tilde{\sigma} \, \tilde{\varepsilon}_t] \tag{25}$$

$$\frac{dB}{d\tilde{t}} = \tilde{H} \left|\frac{d}{d\tilde{t}} [\tilde{\sigma} \, \tilde{\varepsilon}_t]\right| \operatorname{sgn}\left[\frac{d|\tilde{\varepsilon}_t|}{d\tilde{t}}\right] \tag{26}$$

where $\dot{\tilde{\sigma}}$ indicates $d\tilde{\sigma}/d\tilde{t}$, and similarly for $\dot{\tilde{\epsilon}}_e$, $\dot{\tilde{\epsilon}}_v$, $\dot{\tilde{\epsilon}}_t$, and $\dot{\tilde{R}}$. Upon substituting Eqs.(22)-(24) in Eq. (1) expressed in dimensionless form, the following equation is obtained:

$$\dot{\tilde{\sigma}} = 1 - \left[\tilde{\sigma}^N + \left[\frac{\tilde{\sigma} - \tilde{R}}{B} \right]^N \right] \tag{27}$$

Eqs. (24)-(27) can be integrated with the initial conditions of zero dimensionless stress and transient strain. As steady state is reached, i.e., the dimensionless stress rate and transient strain rate decay to zero, the above equations show that the dimensionless stress and transient strain tend to one and 1/A, respectively. The stress at steady state will therefore attain the value of σ_{min} given by Eq. (21). A single master curve can be used to relate the dimensionless stress and time since the temperature dependent constant V and the applied strain rate have been eliminated from the equations. Experimental data is currently unavailable for verifying the dimensionless relationships under constant strain rate loading.

Closed-Form Analytical Solutions for Creep and Recovery Response.-- As previously stated, closed form analytical solutions exist for creep and recovery response when isotropic hardening is absent, i.e., B is a constant. These solutions are valuable since they provide insights regarding the behavior of the model. The analytical solutions are derived below.

In an ideal creep test the stress, σ, is applied instantaneously and the stress rate history is a Dirac delta function, $\delta(t)$, with amplitude σ. This history is zero for all t except at t=0 where it is infinity such that:

$$\int_{-\infty}^{t^*} \sigma \, \delta(t) = \sigma \tag{28}$$

for $t^* > 0$ and zero otherwise. Consequently, the initial strain rate predicted by the model is also a Dirac delta function, i.e., it is equal to infinity. The amplitude of this function is σ/E, which when integrated in a manner similar to Eq. (28) corresponds to the instantaneous elastic strain. For time incrementally greater than zero, the strain rate is finite and equals:

$$\dot{\varepsilon}^{+} = (\sigma/BV)^N + (\sigma/V)^N \tag{29}$$

Equation (29) recognizes that the elastic back stress in Eq. (5) is equal to zero initially. Since the first term of the equation which represents transient flow dominates the initial creep response, the constant B will generally be less than one.

The dimensionless creep compliance function for the model, J, is the sum of the dimensionless elastic, transient and viscous strains, respectively, i.e.

$$J = \tilde{\varepsilon}_e + \tilde{\varepsilon}_t + \tilde{\varepsilon}_v \tag{30}$$

The dimensionless elastic and viscous strains are given in Eqs. (12) and (13). The dimensionless transient strain can be analytically derived from Eqs. (15) and (16) with a substitution of variables approach. In particular, define a variable q as follows:

$$q = 1 - A\,\tilde{\varepsilon}_t \tag{31}$$

Then,

$$\dot{q} = -A\,\dot{\tilde{\varepsilon}}_t \tag{32}$$

Substitution of Eqs. (31) and (32) into Eq. (15) and a separation of variables yields:

$$\int \frac{dq}{q^N} = \frac{-A}{B^N} \int d\tilde{t} \tag{33}$$

Integrating Eq. (33), applying the initial condition of $\tilde{\varepsilon}_t = 0$, i.e., q = 1, and substituting for q results in:

$$\tilde{\varepsilon}_t = 1/A - [\ A^{N-1} + A^N/B^N(N-1)\tilde{t}\,]^{1/(1-N)} \tag{34}$$

Equation (30) together with Eqs. (12), (13) and (34) provide a closed form analytical solution for the dimensionless creep compliance function. Also, by substituting Eq. (34) in Eq. (15), the dimensionless transient strain rate can be expressed in terms of dimensionless time as:

$$\dot{\tilde{\varepsilon}}_t = [B^{N-1} + A/B(N-1)\tilde{t}\,]^{N/(1-N)} \tag{35}$$

Equations (34) and (35) show that the dimensionless transient strain and strain rate tend to 1/A and $1/B^N$ as dimensionless time tends to infinity and zero, respectively.

If creep recovery is allowed to occur at time $\tilde{t}=\tilde{t}_u$, the elastic component of the strain is recovered instantaneously while the viscous component is irrecoverable and remains unchanged with time. However, the transient strain will decay with time according to the following closed form analytical solution that can be derived from Eqs. (15) and (16) in a manner similar to Eq. (34):

$$\tilde{\varepsilon}_t = [\tilde{\varepsilon}_{tu}^{\,1-N} + (A/B)^N(N-1)(\tilde{t}-\tilde{t}_u)]^{1/(1-N)} \tag{36}$$

where $\tilde{\varepsilon}_{tu}$ is the dimensionless transient strain at the time of unloading. Equation (36) shows that the dimensionless transient strain decays to zero with dimensionless time after unloading.

3. EXPERIMENTAL VALIDATION OF UNIAXIAL MODEL

This section first identifies the uniaxial model parameters and discusses methods for determining them. Then, model predictions under constant stress loading are verified against the experimental data of Jacka (1984) and Sinha (1978). The model is also compared with Sinha's (1979) predictions for the relative contribution of transient strain to the total strain during creep. To further demonstrate the capability of the model, the predicted strain response under a monotonically increasing stress history is verified against Sinha's (1981) test data. Finally, the creep and recovery response of randomly oriented snow ice is studied using Brill and Camp's data taken from Sinha (1979).

Parameter Identification and Estimation.-- The uniaxial model contains a total of six parameters: E, N, V_o, A, H and B_o. For single ice crystals and transversely isotropic ice, five independent elastic moduli are needed to describe elastic behavior. Values for these elastic moduli are available for single crystals (see for example, Green and Mackinnon, 1956). The value of E for polycrystalline isotropic ice can be estimated fairly well from the elastic moduli of single crystals (Gammon et al., 1983). Typical values of E for isotropic polycrystalline ice are given in Section 2 of this paper.

Based on the results of tests by a number of researchers carried out at -10°C in the stress range 0.1 to 2 MPa, Ashby and Duval (1985) have estimated the value of N to be three for the creep of isotropic polycrystals and two for the basal glide of monocrystals. The use of N=3 for isotropic polycrystalline ice at moderate stresses is supported by theoretical models which assume dislocation mobility as the rate-controlling process (Baker, 1982). Sinha (1978) has also suggested the same value for the stress exponent in his equation for the viscous creep of polycrystalline ice.

The temperature independent constant V_o and the activation energy Q can be estimated from creep data for various temperatures. From the values of the parameters used in Sinha's equation (1978, 1979), V_o is estimated to be 6.59×10^{-3} MPa $s^{1/N}$ for Q=67 KJ mol^{-1}.

Under constant stress loading, the parameters A and B_o determine the maximum value of the transient strain (σ/AE) and the initial transient strain rate $(\sigma/B_oV)^N$, respectively. The constant A can be estimated by subtracting the elastic strain and the viscous strain from the total strain when steady state is reached. Since the total recoverable deformation is $\sigma/E+\sigma/AE$, the fully relaxed modulus, equal to the applied stress per unit maximum recoverable deformation, is given by EA/(1+A). This allows A to be computed from a creep recovery test as well. The constant B_o can be estimated from Eq. (29). This requires knowledge of the initial strain rate and the constant V. The latter can be computed from Eq. (4), but initial strain rates derived from the measured initial strains may be somewhat inaccurate since experimental measurements of small strains tend to be unreliable (Jacka, 1984, Mellor and Cole, 1982). The parameter H controls the amount of isotropic hardening at a given time. It can be estimated from creep strain and strain rate data using Eq. (5). Having determined V, the viscous strain and strain rate histories are known, and the transient strains and strain rates can then be extracted from the creep data. Noting Eqs. (6) and (7), Eq. (5) can be written in the following way:

$$\ln[\sigma - AE\varepsilon_t - B_o V\dot{\varepsilon}_t^{1/N}] = \ln H + \ln [V\varepsilon_t \dot{\varepsilon}_t^{1/N}] \qquad (37)$$

The quantity on the left-hand side plotted against the second term on the right-hand side of Eq. (37) is a straight line and H can be computed from its intercept with the y-axis.

Comparisons of the model predictions with experimental data in this paper is based on the following values for N, E, V_o and Q:

$N = 3$
$E = 9500$ MPa
$V_o = 6.59 \times 10^{-3}$ MPa $s^{1/N}$
$Q = 67$ kJ mol^{-1}

<u>Comparison of Model Predictions with Jacka's Creep Data.</u>-- Jacka (1984) has published results of uniaxial compression tests on isotropic polycrystalline ice with a mean grain size of 1.7±0.2 mm. The samples were tested under constant stress ranging from 0.1 to 1.5 MPa at the following specific temperatures: -5.0, -10.6, -17.8 and -32.5°C. Figs. 1, 2 and 3 show plots for Jacka's data (taken from Ashby and Duval, 1985) corresponding to $\tilde{\varepsilon}$ versus $\tilde{t}$, $\tilde{\dot{\varepsilon}}$ versus $\tilde{t}$, and $\tilde{\dot{\varepsilon}}$ versus $\tilde{\varepsilon}$, respectively. The predictions of the model, obtained by solving Eqs. (15)-(17) are indicated by solid lines with A=0.017, B_o=0.24 and $\tilde{H}$= 0.024. Also shown are the model predictions for no isotropic hardening,

i.e., solutions provided by Eqs. (12)-(14) and Eqs. (34)-(35). Parameters used for generating these curves are A=0.033 and B=0.402. Note that for experimental data plotted in dimensionless form, the model predictions using Eqs. (12)-(17) as well as Eqs. (34)-(35) are independent of E, V_o and Q. Ashby and Duval (1985) have modified Sinha's equation for creep to a form which satisfies the dimensional requirements. The predictions of the modified equation are also shown in the figures. In referring to Jacka's data it is understood that all variables are normalized and the word dimensionless is dropped when referring to them.

The solid lines show that agreement between model predictions and data is good when strain rate is plotted against time or strain (Figs. 1 and 2). The predicted master curve in the strain versus time plot (Fig. 3) represents the data well, but at small times the predicted strains somewhat overestimate the experimental data. With no isotropic hardening, the strain rates are underestimated while the strains agree well with data. On the other hand, the modified equation provides a good prediction of the strain rate versus time response (Fig. 1), but it over-predicts the initial strains (Figs. 2 and 3) in spite of a factor of two reduction in the value of the parameter (parameter A in Ashby and Duval's paper) which equals the maximum transient strain.

Comparison of Model Predictions with Sinha's Creep Data.-- Sinha (1978) has conducted tests on the creep behavior of transversely isotropic columnar-grained ice (S-2 ice) with an average grain diameter of 3 mm. The tests were conducted in the temperature range of -9.9 to -41°C under a uniaxial compressive load of 0.49 MPa acting in the plane of transverse isotropy. Based on the observations that the activation energy for both viscous flow and transient deformation appears to be equal and that Young's modulus is relatively independent of temperature, Sinha (1978) postulated that the time dependence of the strain at one temperature can be obtained by shifting the measured dependence at another temperature along the time scale using a shift function. Figure 4 shows the creep strains obtained at various temperatures shifted to a reference temperature of -10°C. The solid line indicates the model prediction with A=0.33, B_o=0.058 and $\tilde{H}$=0.63. The value of A is identical to that obtained by Sinha (1978).

The agreement between the experimental data and theoretical results is very good. Notice also that the values of A, $\tilde{H}$ and B_o used for Sinha's and Jacka's data are different, reflecting differences in the ice types that were tested, i.e., isotropic and granular versus transversely-isotropic and columnar-grained, and the average diameters of ice grains. Such modifications to parameter values are also needed for Sinha's equation. For example, the parameter corresponding to A was determined to be 1/3 from Sinha's tests on ice with a grain size of 3 mm, but values of 1/70 and 1/35 were found to be suitable for Jacka's data (Ashby and Duval, 1985).

Model Prediction of Ratio of Transient to Total Strain.-- The parameter AE can be interpreted as an anelastic modulus (not to be confused with relaxed modulus), while BV represents the resistance to transient flow. If transient deformation is related to grain size as postulated by Sinha (1979), then the parameters A and H will depend on grain size. Sinha's (1979) model considers both transient strain and strain rate to be inversely proportional to grain size. For consistency with this formulation, it is necessary for the model parameters to be related to the grain size d as follows:

$$A = d/A' \tag{38}$$

$$B_o = B_o' d^{(1/N)} \tag{39}$$

$$\tilde{H} = \tilde{H}' \, d^{(2/N)} \tag{40}$$

where A', B_o' and $\tilde{H}$' are grain size independent material parameters. The values of these latter parameters are calculated from Eqs. (38)-(40) respectively. For the previously determined values of A, B_o and $\tilde{H}$ (viz., 0.33, 0.058 and 0.63) A'=9 mm, B_o'=0.04 $mm^{-1/N}$, and H'=0.3 $mm^{-2/N}$.

The analytical solutions for the case of no isotropic hardening are useful for inferring some of the characteristics of the complete model. It is apparent from Eqs. (14) and (35) that the ratio of the (dimensionless) transient strain rate to the viscous strain rate decreases with increase in grain size. The ratio also decreases with dimensionless time (Eq. 35). According to the definitions of dimensionless time (Eq. (10)) and viscous strain rate (Eq. (3)), the ratio must also decrease with increase in applied stress. These trends are in agreement with predictions of Sinha's equation.

The predictions of the proposed model and Sinha's equation with regard to the relative contribution of transient strain to total strain are compared below. Let the ratio of the transient strain to the total strain, γ, be defined as follows:

$$\gamma = \frac{\tilde{\varepsilon}_t}{\tilde{\varepsilon}} = \frac{\tilde{\varepsilon}_t}{\tilde{\varepsilon}_t + \tilde{t} + 1} \tag{41}$$

where the dimensionless variables have been defined previously. By solving Eqs. (15)-(17) the strain dependence of γ under a constant stress load of 1 MPa at -10°C for various grain sizes is predicted as shown in Fig. 5. The important features predicted by Sinha's equation such as the increasing value of γ with decreasing d, the occurrence of maximum γ at small strains, the gradual shift of the maxima towards larger strains with decreasing d, the gradual decrease in γ with increase in strain after the peak is passed, and the decreasing effect of d on γ at large strains are also observed in Fig. 5, although the numerical values are different.

Furthermore, since the relationship between the dimensionless transient strain and time is independent of temperature (Eq. (34)), it can be deduced from Eq. (41) that the evolution of γ with dimensionless strain for a given grain size is unique, i.e., independent of both temperature and stress level. Recalling that dimensionless strain is equal to $\varepsilon E/\sigma$ and if E does not change appreciably with temperature, then for a given grain size, the evolution of γ with strain (stress) itself is independent of temperature but not of stress (strain). This is also predicted by Sinha's equation.

Prediction of Model Response Under Monotonically Increasing Stress.-- The rate sensitivity of the compressive strength of columnar-grained ice under constant cross-head displacement rates has been investigated by Sinha (1981). It was shown that the results are representative of the constant stress rate rather than the constant strain rate condition. A numerical integration method, based on a generalized creep equation and the principle of superposition, was developed by Sinha (1983) to predict the evolution of strain corresponding to a given stress history.

For the proposed model, the strain response can be obtained by numerically integrating Eqs. (1)-(7). In this example, the actual stress-time history (not the constant stress rate idealization) is taken as input and is known from Sinha's (1981) tests on ice with an average grain size of 4.5 mm. The tests were carried out at -10°C under a constant cross-head displacement rate of 1.25×10^{-3} cm/s. The values of the hardening parameters are determined from Eqs. (38)-(40) for the given grain size and previously determined values of the grain size independent parameters.

The stress-time data is presented in the upper curve of Fig. 6b, while the lower curve shows the predicted strain-time response superimposed on the test data. The agreement between theory and experiment is quite good, given that the parameter values which were determined from a different data set are unchanged. Figure 6a shows that when stress is plotted against strain, a very good representation of the data is obtained. It is possible to conclude from this figure that the predictions of the proposed model under monotonically increasing stress compare well with experimental data.

Comparison of Model Predictions with the Creep and Recovery Data of Brill and Camp.-- Figure (7) shows creep and recovery data for tests conducted on randomly oriented snow ice by Brill and Camp (reproduced in Sinha, 1979.) The three sets of data refer to tests carried out under the following conditions: curve

(a) at -5°C and 0.232 MPa, curve (b) at -5°C and 0.125 MPa, and curve (c) at -10°C and 0.238 MPa. The model predictions, shown in solid lines, are generated with A'=6.5 mm, B_o'=0.11 $mm^{-1/N}$ and $\tilde{H}'$=0.01 $mm^{-2/N}$. The grain sizes used for curves (a), (b) and (c) are 2 mm, 2.3 mm, and 1.5 mm respectively, which are almost identical to the values determined by Sinha (1979). Differences in the hardening parameters reflect the difference in ice types, i.e., transversely isotropic and columnar-grained versus isotropic and granular snow ice. The agreement between model predictions and test data is quite good, given that the measurement of strain recovery in ice shows large scatter (Sinha, 1982.)

A major difference exists between Sinha's recovery model and the present formulation. The former can result in a decrease of the permanent/irrecoverable viscous strain and eventually lead to reversed strain (e.g., an elongation or tensile strain due to recovery from compressive creep). This is due to the particular form of the superposition principle adopted, in which the elastic and the transient strains resulting from the stress drop are subtracted from the total strain at unloading. Recovery is thus the mirror image of the transient term in the equation for loading and as time increases it can exceed the transient creep strain at the instant of unloading. In order to overcome the problem, the superposition principle is not used when the predicted strain during recovery becomes less than the accumulated viscous strain and the strain is kept fixed thereafter at a value equal to that of the viscous strain at unloading. The proposed theory does not suffer from this modeling limitation since the values of R and B decrease during unloading, reflecting creep recovery.

4. MULTIAXIAL MODEL FORMULATION

Natural ice has very complex crystalline and stratigraphic structures, and generally cannot be considered as an isotropic material. For example, columnar fresh-water ice may have two sources of anisotropy: (a) the c-axis may be oriented perpendicular to the axis of crystal growth, and (b) the c-axes of different crystals may show preferred orientation in the plane on which they lie. According to the classification of Michel and Ramseier (1971), the first source of anisotropy is exhibited by S2 ice while both types of anisotropy are present in S3 ice.

The anisotropy of ice strongly influences its mechanical behavior. Carter and Michel (1971) have tested S2 ice at -10°C under constant strain rate loading conditions. They find that the first source of anisotropy leads to a vertical to horizontal maximum stress or strength ratio of about two. Information on the effect of the second source of anisotropy on the strength ratio of freshwater ice is currently unavailable, although data for sea ice indicates the following strength ratios: (a) 0.25-0.60 for strength at a 45 degree azimuthal angle to that along the c-axes, and (b) 0.50-0.95 for strength at a 90 degree angle to that along the c-axis (Peyton, 1968; Vittoratos, 1979; Wang, 1979; Richter-Menge et al., 1985).

Theoretical formulations which account for anisotropy in ice with a transversely isotropic model have been developed by Reinicke and Ralston (1977) and by Vivatrat and Chen (1985). The former model is based on plasticity theory and considers ice to be a pressure sensitive material as well. The latter is a pressure insensitive, elastic - power law creep formulation.

The development presented here is based on an orthotropic generalization (i.e., the general case of a material having three orthogonal planes of symmetry) of the proposed uniaxial model which accounts for both transient and steady state flow in ice. The transversely isotropic and isotropic formulations are special cases of the orthotropic generalization.

Conceptual Framework and Constraint Conditions.-- The three-dimensional generalization of the model follows naturally from the uniaxial formulation, i.e., it is based on strain decomposition, linear elasticity and the rate theory of flow. Constitutive relations are derived for each mechanism of deformation in the model, resulting in the orthotropic equivalent of Eqs. (1)-(7).

To model orthotropic elasticity, the classical formulation from elasticity theory is adopted (see, for example, the book by Lekhnitskii, 1963). Compressibility of ice deformation is implicitly contained in linear elasticity where the Poisson's ratios are less than 0.5, while the transient and viscous deformation-rate mechanisms are assumed to be incompressible (Palmer, 1967, Sinha, 1987). The orthotropic generalization of the viscous deformation-rate mechanism is derived from the rate theory of flow by applying the normality principle to a scalar valued flow potential expressed in terms of an equivalent stress measure for incompressible orthotropic materials. Similarly, the derivation of the orthotropic constitutive relations for transient flow are based on the normality of the stress difference vector $\underline{\sigma} - \underline{R}$ to a scalar valued flow potential expressed in terms of an equivalent stress difference measure. Evolution equations for the back stress vector $\underline{R}$ and the equivalent drag stress B_{eq} follow from the uniaxial equations.

The total, elastic, viscous and transient strain rate vectors must obey the following constraint condition:

$$\dot{\underline{\varepsilon}} = \dot{\underline{\varepsilon}}_e + \dot{\underline{\varepsilon}}_v + \dot{\underline{\varepsilon}}_t \tag{42}$$

where the strain rates are in engineering notation, for example, $\dot{\underline{\varepsilon}} = [\dot{\varepsilon}_{xx}\ \dot{\varepsilon}_{yy}\ \dot{\varepsilon}_{zz}\ \dot{\gamma}_{xy}\ \dot{\gamma}_{yz}\ \dot{\gamma}_{zx}]^T$. The superscript T denotes the transpose of vectors and matrices. For convenience, the stress difference $\underline{\sigma}-\underline{R}$ is denoted by the symbol $\underline{\sigma}_d$, i.e.:

$$\underline{\sigma}_d = \underline{\sigma} - \underline{R} \tag{43}$$

The stress vectors are also expressed in engineering notation.

Orthotropic Model of Elasticity.-- The constitutive relation between the elastic strain and the stress is described in rate form as:

$$\dot{\underline{\varepsilon}}_e = \underline{C}\ \dot{\underline{\sigma}} \tag{44}$$

where $\underline{C}$ is the compliance matrix for a linearly elastic but orthotropic material. Values of the Young's moduli, Poisson's ratios and shear moduli for orthotropic and transversely isotropic polycrystalline ice are not readily available. However, engineering approximations involving a weighted average of the five elastic constants for single crystals have been developed (Gammon et al., 1983, Ashton, 1986). The Poisson's ratio for isotropic polcrystalline ice is approximately 0.3 (Gold, 1977).

Orthotropic Model of Viscous Flow.-- To derive the relationship between the viscous strain rate vector $\underline{\dot{\epsilon}}_v$ and the stress vector $\underline{\sigma}$, an equivalent stress measure generalized for pressure insensitive orthotropic materials, i.e., with identical behavior in tension and compression, is defined:

$$\sigma_{eq}^2 = \frac{3}{\beta}\left[\frac{a_1}{3}(\sigma_{xx}-\sigma_{yy})^2 + \frac{a_2}{3}(\sigma_{yy}-\sigma_{zz})^2 + \frac{a_3}{3}(\sigma_{zz}-\sigma_{xx})^2 + 2a_4\sigma_{xy}^2 + 2a_5\sigma_{yz}^2 + 2a_6\sigma_{zx}^2\right] \tag{45}$$

with β chosen to be (a_1+a_2) so that $\sigma_e=\sigma_{yy}$ when the stress components are described by the vector $\underline{\sigma} = [0\ \sigma_{yy}\ 0\ 0\ 0\ 0]^T$, i.e., the y-axis is chosen as the reference direction. Equation (45) is similar in form to that used by Hill (1950) for metal plasticity and may be expressed in compact form using matrix notation as:

$$\sigma_{eq}^2 = 3/\beta\ \ \underline{\sigma}^T\ \underline{G}\ \underline{\sigma} \tag{46}$$

where

$$\underline{G} = \begin{bmatrix} \frac{a_1+a_3}{3} & \frac{-a_1}{3} & \frac{-a_3}{3} & & \underline{0} & \\ & \frac{a_1+a_2}{3} & \frac{-a_2}{3} & & & \\ & & \frac{a_2+a_3}{3} & & & \\ & \text{SYMMETRIC} & & 2a_4 & & \\ & & & & 2a_5 & \\ & & & & & 2a_6 \end{bmatrix} \tag{47}$$

The viscous strainrate vector can now be related to the stress vector by defining a scalar valued viscous flow potential function:

$$\phi_v = a \frac{\sigma_{eq}^{N+1}}{N+1} \tag{48}$$

which obeys the normality principle:

$$\underline{\dot{\varepsilon}}_v = \frac{\partial \phi_v}{\partial \underline{\sigma}} \tag{49}$$

The parameter a in Eq. (48) is a constant associated with the power law for uniaxial loading in the y-direction; it is equivalent to the quantity $1/V^N$ in Eq. (3). Combining Eqs. (46)-(49) yields the desired relationship:

$$\underline{\dot{\varepsilon}}_v = \lambda \, \underline{S}^* \tag{50}$$

where

$$\lambda = 3/\beta \; a \; \sigma_{eq}^{N-1} \tag{51}$$

and

$$\underline{S}^* = \underline{G} \; \underline{\sigma} \tag{52}$$

Note that $\underline{S}^*$ is a pseudo-deviatoric stress vector for orthotropic materials. If a_1 to $a_6 = 1$, $\underline{S}^*$ reduces to the conventional deviatoric stress vector, σ_{eq} reduces to the conventional equivalent stress measure for isotropic materials, and Eq. (50) becomes the well known three-dimensional generalization of the power law for creep of isotropic materials, as presented by Palmer (1967) for glacier flow.

Using the hypothesis of energy equivalence, the relationship between the equivalent stress defined in Eq. (45) and an equivalent strain rate measure can be established. The rate of dissipation of energy per unit volume, P, is given by:

$$P = \underline{\sigma}^T \; \underline{\dot{\varepsilon}}_v \tag{53}$$

Application of this hypothesis yields:

$$\underline{\sigma}^T \, \dot{\underline{\varepsilon}}_v = \sigma_{eq} \, \dot{\varepsilon}_{v,eq} \tag{54}$$

where $\dot{\varepsilon}_{v,eq}$ is the equivalent viscous strainrate. The viscous strain rate vector in Eq. (54) can be eliminated using Eqs. (50), (52) and (46) in succession to yield:

$$\dot{\varepsilon}_{v,eq} = a \, \sigma_{eq}^{N} \tag{55}$$

Given the equivalent stress measure, Eq. (55) can be used to compute the equivalent viscous strain rate. Alternatively, an explicit expression can be derived by first eliminating $(\sigma_{xx} - \sigma_{yy})^2, \ldots, \sigma_{zx}^2$ in Eq. (45) through the use of Eq. (50) and then substituting the resulting expression for σ_{eq} in Eq. (55). The final expression can be expressed in compact notation as follows:

$$\dot{\varepsilon}_{v,eq}^{2} = \beta/3 \; \dot{\underline{\varepsilon}}_v^T \, \underline{H} \, \dot{\underline{\varepsilon}}_v \tag{56}$$

where the transformation matrix $\underline{H}$ is given by:

$$\underline{H} = \begin{bmatrix} \frac{3(a_1+a_3)a_2^2}{a^{*2}} & \frac{-3a_1a_2a_3}{a^{*2}} & \frac{-3a_1a_2a_3}{a^{*2}} & & & \\ & \frac{3(a_1+a_2)a_3^2}{a^{*2}} & \frac{-3a_1a_2a_3}{a^{*2}} & & \underline{0} & \\ & & \frac{3(a_2+a_3)a_1^2}{a^{*2}} & & & \\ & & & 2/a_4 & & \\ & \text{SYMMETRIC} & & & 2/a_5 & \\ & & & & & 2/a_6 \end{bmatrix} \tag{57}$$

with $a^* = a_2a_3+a_3a_1+a_1a_2$. It is apparent that Eq. (56) can be reduced to the conventional equivalent strain rate measure for isotropic materials if a_1 to $a_6 = 1$. Moreover, when loading is in the reference direction, $\dot{\varepsilon}_{v,eq} = \dot{\varepsilon}_{v,yy}$, and Eq. (55) reduces to uniaxial loading in the reference direction.

<u>Orthotropic Model of Transient Flow.</u>-- The orthotropic generalization of the transient deformation is based on the assumption of flow incompressibility. Although this may not be

strictly true, Sinha (1987) has argued that transient flow does not change the volume appreciably and that the assumption is valid. This assumption is implicitly made for metals (Hart, 1976). A second assumption is that the orthotropy is described by the same set of parameters, i.e., a_1 through a_6.

The model accounts for isotropic hardening as well as kinematic or directional hardening, which leads to subsequent deformation or stress-induced anisotropy (as opposed to material or texture anisotropy). The relationship between the transient strain rate $\underline{\dot{\varepsilon}}_t$ and the stress vector $\underline{\sigma}_d$ can be derived from the normality of $\underline{\sigma}_d$ to a scalar valued transient flow potential function. Following the procedure used to derive Eqs. (50)-(52) yields:

$$\underline{\dot{\varepsilon}}_t = 3/\beta \; a/B_{eq}{}^{N} \; \sigma_{d,eq}{}^{N-1} \; \underline{S}_d{}^{*} \tag{58}$$

where

$$\underline{S}_d{}^{*} = \underline{G} \; \underline{\sigma}_d = \underline{G} \; \underline{\sigma} - \underline{G} \; \underline{R} \tag{59}$$

B_{eq} is the equivalent nondimensional drag stress, and $\sigma_{d,eq}{}^2 = 3/\beta \; \underline{\sigma}_d{}^T \; \underline{G} \; \underline{\sigma}_d$. To complete the multiaxial formulation, the evolution equations for $\underline{R}$ and B_{eq} as well as the value of the eqivalent stress difference measure are required.

For consistency with the incompressiblilty constraint on transient flow and the elastic nature of back stresses, it is necessary to define a scalar valued flow potential in terms of the equivalent back stress, $R_{eq}{}^2 = 3/\beta \; \underline{R}^T \; \underline{G} \; \underline{R}$, i.e.,

$$\phi_s = b/2 \; R_{eq}{}^2 \tag{60}$$

where b equals 1/AE in the reference direction. The transient strain can then be related to the pseudo-deviatoric back stress vector by imposing normality:

$$\underline{\varepsilon}_t = \frac{\partial \phi_s}{\partial \underline{R}} = \frac{3}{\beta} \; b \; \underline{S}_R{}^{*} \tag{61}$$

where

$$\underline{S}_R^* = \underline{G}\ \underline{R} \tag{62}$$

The evolution equation for the back stress vector is the time derivative of Eq. (61), i.e.,

$$\dot{\underline{S}}_R^* = \underline{G}\ \dot{\underline{R}} = \beta/(3b)\ \dot{\underline{\varepsilon}}_t \tag{63}$$

The equivalent non-dimensional drag stress B_{eq} is given by:

$$\dot{B}_{eq} = c\ \ \dot{\varepsilon}_{t,eq}\ \ \mathrm{sgn}\left[\frac{d\varepsilon_{t,eq}}{dt}\right] \tag{64}$$

where c equals H in the reference direction. Both the equivalent transient strain rate and strain measures in Eq. (64) can be obtained using the transformation matrix $\underline{H}$, derived in Eq. (57) for the equivalent viscous strain rate.

The equivalent stress difference can be expressed as a function of the equivalent transient strain. Noting that $\sigma_{d,eq}{}^2$ can be defined in terms of $\underline{S}_d{}^*$ as $3/\beta\ \underline{\sigma}_d{}^T\ \underline{S}_d{}^*$, and substituting $\underline{S}^*-\underline{S}_R{}^*$ for $\underline{S}_d{}^*$ and $\underline{\sigma}-\underline{R}$ for $\underline{\sigma}_d$ yields:

$$\sigma_{d,eq}{}^2 = 3/\beta\ [\underline{\sigma}^T\underline{S}^* - 2\ \underline{\sigma}^T\ \underline{S}_R{}^* + \underline{R}^T\underline{S}_R{}^*] \tag{65}$$

$\underline{\sigma}$ and, consequently, $\underline{S}^*$ may be considered as given, while $\underline{S}_R{}^*$ may be computed by integrating Eq. (63). Substitution of Eq. (61) in the last term of Eq. (65) yields $(\beta/3b)\ \underline{R}^T\underline{\varepsilon}_t$, where $\underline{R}^T\underline{\varepsilon}_t$ equals twice the elastic strain energy stored in the material. Based on an equivalence in the rate of stored elastic strain energy, it follows that:

$$\underline{R}^T\ \dot{\underline{\varepsilon}}_t = R_{eq}\ \dot{\varepsilon}_{t,eq} \tag{66}$$

The equivalent uniaxial relationship between R_{eq} and $\varepsilon_{t,eq}$ is given by:

$$\dot{R}_{eq} = 1/b\ \dot{\varepsilon}_{t,eq} \tag{67}$$

since b=1/AE. Equation (67) and the right-hand-side of Eq. (66) are integrated simultaneously with respect to time to yield $\underline{R}^T \underline{\varepsilon}_t$. On substitution in Eq. (65), the following result is obtained:

$$\sigma_{d,eq}^{2} = 3/\beta\ \underline{\sigma}^T \underline{S}^* - 2/b\ \underline{\sigma}^T \underline{\varepsilon}_t + (\varepsilon_{t,eq}/b)^2 \tag{68}$$

The second term in this equation is obtained by substituting Eq. (61) in the corresponding term of Eq. (65).

Equations (42), (44), (50), (58), (63) and (64) are the orthotropic counterparts of Eqs. (1)-(3) and (5)-(7). They form the governing equations that can be integrated numerically to predict the model response under variable loading histories involving multiaxial states of stress.

5. EXPERIMENTAL VALIDATION OF MULTIAXIAL MODEL

Estimation of Orthotropic Model Parameters.-- The orthotropic model parameters can be estimated from experimental data under steady viscous flow conditions. Five uniaxial (compression) tests are required to obtain the five parameters a_2 through a_6 since a_1 can be set to one without loss of generality. In a comprehensive paper reviewing the constants used in Glen's power law for polycrystalline glacier ice, Hooke (1981) has concluded that in the absence of experimental evidence to the contrary, a value of three for the power law index N is reasonable, irrespective of the "structural state", e.g., fabric and grain size. The effect of the structural state is then accounted for by changing the "viscosity" parameter (V in the present model). This is the approach adopted here, in which N is three and the initial texture or material anisotropy is accounted for through the use of an appropriate equivalent stress measure. Under uniaxial loading in any specific direction, the viscosity parameter relating viscous strain rate and stress in the specified direction is provided by Eq. (55), the definition for the equivalent stress in Eq. (45), and the definition for the equivalent viscous strain rate in Eq. (56).

The x-axis is taken to be normal to the ice sheet which is defined by the y-z plane. The c-axes of the ice crystals are assumed to lie in the y-z plane and are aligned in the y-direction. The tests are conducted in three orthogonal directions y, x, and z respectively, and along the three 45° axes on the y-z, x-y, and z-x planes respectively. Let β_1 to β_5 represent the experimentally determined ratios of the maximum stresses (strengths) for the latter five tests, respectively, to the maximum stress in the reference y-direction for tests conducted at the same constant strain rate. In the case of creep tests, the β's represent inverse ratios of the corresponding minimum strain rates raised to the power of 1/N. The parameters a_2 to a_6 may be determined from the following equations (see Appendix A for derivations):

$$a_2 = - \frac{\beta_1{}^n - \beta_2{}^n (1-\beta_1{}^n)}{\beta_1{}^n - \beta_2{}^n (1+\beta_1{}^n)} \tag{69}$$

$$a_3 = - \frac{\beta_1{}^n + \beta_2{}^n (1-\beta_1{}^n)}{\beta_1{}^n - \beta_2{}^n (1+\beta_1{}^n)} \tag{70}$$

$$a_4 = \beta/6 \; [4\beta_4{}^{-n} - \beta_2{}^{-n}] \tag{71}$$

$$a_5 = \beta/6 \; [4\beta_3{}^{-n} - \beta_1{}^{-n}] \tag{72}$$

$$a_6 = \beta/6 \; [4\beta_5{}^{-n} - 1] \tag{73}$$

where n=2N/(N+1). Typical values for β_1 lie between 2-5. While the values of the constants β_2 to β_5 are not generally available in the literature for pure polycrystalline ice, they may be estimated from the sea ice data referred to in the beginning of Section 4.

For a transversely isotropic material, i.e., isotropy in the y-z plane, $\beta_2=\beta_3=1$ and $\beta_4=\beta_5$. As a result, $a_1=a_3=1$, $a_4=a_6$, the parameters a_2 and a_5 are functions of only β_1, while a_4 depends on both β_1 and β_4. Only two uniaxial tests are required to obtain β_1 and β_4: one in the x-direction and one along the 45° axis on the x-y or z-x planes.

<u>Model Predictions Under Steady State Plane-Strain and Triaxial Compressive Loadings.</u>-- Experimental data on the pure flow (both transient and steady state) of polycrystalline ice under multiaxial states of stress is unavailable, although the incompressible and istropic power law of Palmer (1967) is widely used to describe the deformation of glacier ice under such stresses. In spite of data limitations, an attempt is made here to evaluate model predictions under steady flow conditions.

Frederking (1977) has conducted plane strain uniaxial compression tests on columnar-grained transversely isotropic freshwater ice. For his type A tests, strains in the z-direction are constrained to zero and stresses are applied in the y-direction. At steady state where the power law orthotropic formulation suffices, the ratio Γ_z of the plane strain stress to the unconfined stress at the same strain rate is directly related to β_1 by the following equation (see Appendix B)

$$\Gamma_z = \left[\frac{4\beta_1^{2n}}{4\beta_1^{n} - 1}\right]^{1/n} \tag{74}$$

The equation predicts Γ_z to vary between 2.1-5.1 for experimentally observed values of β_1 ranging from 2 to 5, and N=3. This is consistent with Frederking's experimental observations which were close to 2 at high strainrates and to 5 at low strain rates. In his type B tests, strains in the x-direction are constrained to zero while stresses are again applied in the y-direction. In this case, the ratio Γ_x is given by:

$$\Gamma_x = \left[1 + \frac{1}{4\beta_1^{n} - 1}\right]^{1/n} \tag{75}$$

Since β_1 is generally greater than one, Γ_x will be less than approximately 1.2 for N=3. For typical values of β_1, the predicted values of Γ_x lies between 1.01 to 1.06. This is consistent with Frederking's experiments which showed negligible influence of x-direction confinement on stresses. Although the derivation in Appendix B determines Γ_z and Γ_x as the ratios of two steady state stresses resulting from viscous flow, considerable damage occurred in Frederking's tests. The accuracy of the predictions are interesting nonetheless. This probably occurs because both the unconfined and partially confined strengths are reduced by damage, and the resulting effect on strength ratios is less significant.

According to the orthotropic model, the ratio Γ_t of the maximum axial stress with a confining pressure equal to τ times the axial stress to the maximum axial stress in the unconfined state at the same strain rate should be given by (see Appendix C):

$$\Gamma_t = \frac{1}{1-\tau} \tag{76}$$

The shear stress (i.e. axial stress minus radial stress) normalized by the unconfined stress is independent of τ or confining pressure for the model and equal to one. The triaxial behavior of pure (non-saline) polycrystalline ice has been studied by Jones (1978). His tests, which were performed at strain rates of 10^{-6} to 5×10^{-3} s-1, indicate up to a factor of two increase in shear stress due to confining pressure. Nadreau and Michel (1986) have reported triaxial tests on freshwater, iceberg and saline ice, and their results confirm that shear strength increases with confining pressure and strain rate. The pressure and strain rate sensitivity of damage in ice, which causes the increase in shear strength with confining pressure and strain rate, is examined in the forthcoming paper by Wu and Shyam Sunder (1988).

6. CONCLUSIONS

This paper presents a multiaxial differential flow law for polycrystalline ice which attempts to model the underlying physical deformation mechanisms active in the material. Instantaneous elasticity is modeled by the classical theory of linear elasticity, while the steady viscous deformation-rate mechanism is described by Glen's power law. On the other hand, the transient deformation-rate mechanism is modeled by the interaction between the soft and hard deformation systems which gives rise to an internal drag stress and a back stress. Increasing drag and back stresses are associated with the phenomena of isotropic and kinematic hardening, respectively. Dimensional requirements identified by Ashby and Duval (1985) are satisfied by the model.

The multiaxial generalization follows from conventional elasticity theory and from the rate theory of flow for the viscous and transient deformation-rates. The rate theory assumes normality of the deformation-rate to a scalar valued flow potential expressed in terms of an equivalent stress measure. History effects are modeled with a hardening multiaxial formulation based on the elastic back stress vector and an equivalent (scalar) drag stress measure. Equations are derived for an orthotropic model of incompressible flow and for estimating the orthotropic parameters from uniaxial test data.

The uniaxial model contains a total of six parameters that can be determined from conventional experimental testing methods for ice. The model is verified against Jacka's (1984), Sinha's (1978), and Brill and Camp's test data on the creep of polycrystalline ice. Predictions of the ratio of transient to total strain agree qualitatively with Sinha's equation if grain size effects are taken into account. The mechanical behavior under monotonically increasing stress is successfully predicted using Sinha's (1983) data obtained from constant displacement rate tests.

For the multiaxial model, experimental verification is made difficult by the lack of data for the pure flow of freshwater polycrystalline (S2 or S3) ice. The model predicts pressure-insensitive behavior under conventional triaxial loading conditions. Also, theoretical predictions agree well with Frederking's (1977) data from constant strain rate tests carried out under plane strain conditions (although it should be noted that his data is for ice with distributed cracks or damage induced by loading, not pure flow.)

7. ACKNOWLEDGEMENTS

The authors would like to acknowledge financial support from the U.S. Army Research Office through MIT's Center for Advanced Construction Technology; BP America through MIT's Center for Scientific Excellence in Offshore Engineeing; and the U.S. Department of the Interior, Minerals Management Service.

REFERENCES

Ashby, M.F. and Duval, P. (1985), The Creep of Polycrystalline Ice, Cold Regions Science and Technology, 11, 285-300.

Baker, R.W. (1982), A Flow Equation for Anisotropic Ice, Cold Regions Science and Technology, 6, 141-148.

Barnes, P., Tabor, D., and Walker, J.C.F. (1971), The Friction and Creep of Polycrystalline Ice, Proceedings Royal Society London A, 324, 127-155.

Carter, D. and Michel, B. (1971), Laws and Mechanisms of Apparent Brittle Fracture of River and Lake Ice (In French), Faculte des Sciences, Universite Laval, Quebec, Report S-22.

Derby, B. and Ashby, M.F. (1987), A Microstructural Model for Primary Creep, Acta Metallurgica, Vol. 35, No. 6, 1349-1353.

Frederking, R. (1977), Plane-Strain Compressive Strength of Columnar-Grained and Granular Snow-Ice, Journal of Glaciology, Vol. 18, No. 80, 505-516.

Le Gac, H. and Duval, P. (1980), Constitutive Relations for the Non-Elastic Deformation of Polycrystalline Ice, Tryde, P. (Ed.), Proceedings of the IUTAM Symposium on the Physics and Mechanics of Ice, Springer, 51-59.

Gammon, P.H., Kiefte, H., Clouter, M.J. and Denner, W.W., (1983), Elastic Constants of Artificial and Natural Ice Samples by Brillouin Spectroscopy, Journal of Glaciology, Vol. 29, No. 103, 433-460.

Glen, J.W. (1955), The Creep of Polycrystalline Ice, Proceedings of the Royal Society of London, Ser. A, Vol. 228, No. 1175, 519-538.

Gold, L.W. (1973), Activation Energy for Creep of Columnar-Grained Ice, In Whalley, E., Jones, S.J. and Gold, L.W. (Eds.), Physics and Chemistry of Ice, Roy. Soc. Canada, Ottawa, 362-364.

Gold, L.W. (1977), Engineering Properties of Fresh Water Ice, Journal of Glaciology, Vol. 19, No. 81, 197-212.

Gold, L.W. (1983), Creep of Columnar-Grained Ice at Low Stress, Annals of Glaciology, 4, 73-78.

Green, R.E. and Mackinnon, L. (1956), Determination of the Elastic Constants of Ice Single Crystals by an Ultrasonic Pulse Method, Journal of the Acoustical Society of America, 28, 1292 p.

Hart, E.W. (1976), Constitutive Relations for the Nonelastic Deformation of Metals, Journal of Engineering Materials and Technology, 96, 193-202.

Hill, R. (1950), The Mathematical Theory of Plasticity, Oxford University Press, London.

Hooke, R.L. (1981), Flow Law for Polycrystalline Ice in Glaciers: Comparison of Theoretical Predictions, Laboratory Data, and Field Measurements, Reviews of Geophysics and Space Physics, Vol. 19, No. 4, 664-672.

Jacka, T.H. (1984), The Time and Strain Required for The Development of Minimum Strain Rates in Ice, Cold Regions Science and Technology, 8, 261-268.

Jones, S.J. (1982), The Confined Compressive Strength of Polycrystalline Ice, Journal of Glaciology, 28, 171-177.

Jordaan, I.J. (1986), Numerical and Finite Element Techniques in Calculation of Ice-Structure Interaction, Proceedings of the IAHR Symposium on Ice, Iowa City, Iowa, Vol. II, 405-440.

Lekhnitskii, S.G. (1963), Theory of Elasticity of an Anisotropic Elastic Body, Holden-Day, Inc., San Francisco.

Mellor, M. and Cole, D.M. (1982), Deformation and Failure of Ice under Constant Stress or Constant Strain-Rate, Cold Regions Science and Technology, 5, 201-219.

Michel, B. and Ramseier, R.O. (1971), Classification of River and Lake Ice, Canadian Geotechnical Journal, Vol. 8, 36-45.

Miller, A. (1976), An Inelastic Constitutive Model for Monotonic, Cyclic, and Creep Deformation: Part 1 - Equations Development abd Analytical Procedures, Journal of Engineering Materials and Technology, 96, 97-104.

Nadreau, J.P. and Michel, B. (1986), Secondary Creep in Confined Ice Samples, Proceedings of the IAHR Symposium on Ice, Iowa City, Iowa, Vol. I., 307-318

Palmer, A.C. (1967), Creep-Velocity Bounds and Glacier-Flow Problems, Journal of Glaciology, Vol. 6, No. 46, 479-488.

Peyton, H.R. (1968) , Ice and Marine Structures, Ocean Industry, Vol. 3, No.3, March 1968, 40-41; Vol. 3, No. 9, September 1968, 59-65; Vol. 3, No. 12, December 1968, 51-58.

Reinicke, K.M. and Ralston, T.D. (1977), Plastic Limit Analysis with an Anisotropic, Parabolic Yield Function, International Journal of Rock Mechanics, Mining Sciences and Geomechanics, 14, 147-154.

Richter-Menge, J.A., Cox, G.F.N, Perron, N., Durell, G. and Bosworth, H. (1985), Triaxial Testing of First-Year Sea Ice, Internal Research Report 877, U.S. Army Cold Regions and

Engineering Laboratory, Hanover, New Hampshire.

Shyam Sunder, S., Ganguly, J. and Ting, S.K. (1987), Anisotropic Sea Ice Indentation in the Creeping Mode, Journal of Offshore Mechanics and Arctic Engineering, Vol. 109, No. 2, 211-219.

Sinha, N.K. (1978), Rheology of Columnar-Grained Ice, Experimental Mechanics, 18(12), 464-470.

Sinha, N.K. (1979), Grain-Boundary Sliding in Polycrystalline Materials, Philosophical Magazine A, 40(6), 825-842.

Sinha, N.K. (1981), Rate Sensitivity of Compressive Strength of Columnar-Grained Ice, Experimental Mechanics, 21(6), 209-218.

Sinha, N.K. (1982), Delayed Elastic Strain Criterion for First Cracks in Ice, In Vermeer, P.A. and Luger, H.J. (Eds.), Proceedings of the IUTAM Conference on Deformation and Failure of Granular Materials, A.A. Balkema Rotterday, 323-330.

Sinha, N.K. (1983), Creep Model of Ice for Monotonically Increasing Stress, Cold Regions Science and Technology, 8, 25-33.

Sinha, N.K. (1987), Effective Poisson's Ratio of Isotropic Ice, Proceedings of the Sixth International Offshore Mechanics and Arctic Engineering Symposium, Vol. IV, 189-195.

Sinha, N.K., Timco, G.W., and Frederking, R. (1987), Recent Advances in Ice Mechanics in Canada, In Chung, J.S., Hallam, S.D., Maatanen, M. , Sinha, N.K., and Sodhi, D.S. (Eds.), Advances in Ice Mechanics - 1987, ASME, Offshore Mechanics and Arctic Engineering Symposium Committee, Houston, Texas, 15-35.

Vivatrat, V. and Chen, V.L. (1985), Ice Load Prediction with the Use of a Rate-Dependent Anisotropic Law, Proceedings of the ASCE Specialty Conference: Arctic '85- Civil Engineering in the Arctic Offshore, San Francisco, California, 942-952.

Vittoratos, E.S. (1979), Existence of Oriented Sea Ice by the Mackenzie Delta, Proceedings of the 5th International Conference on Port and Ocean Engineering under Arctic Conditions (POAC 79), Trondheim, Norway, Vol. 1, August, 1979, 643-650.

Wang, Y.S. (1979), Sea Ice Properties, Proceedings of the Technical Seminar on Alaskan Beaufort Sea Gravel Island Design, Exxon Company, USA, Houston, TX, October 1979.

Wu, M.S. and Shyam Sunder, S. (1988), A Rate and Pressure Sensitive Damage Model for Polycrystalline Ice, In Preparation.

APPENDIX A

Orthotropic Material Parameters (a_1 - a_6)

A.1 Definition of Symbols

The derivation here considers only the power law creep of ice. The parameters a_1 to a_6 and β_1 to β_5 have been defined in the paper. The coefficients a, b_2 to b_6 are the constants for the unaxial power law along the y (reference)-, x- and z-directions, and along the 45° axes on the y-z, x-y and z-x planes respectively. Thus,

$$\dot{\varepsilon}_{yy} = a\ \sigma_{yy}^{N} \tag{A.1}$$

$$\vdots$$

$$\dot{\varepsilon}_{45(zx)} = b_6\ \sigma_{45(zx)}^{N} \tag{A.6}$$

where $\dot{\varepsilon}_{yy},\ldots,\dot{\varepsilon}_{45(zx)}$ and $\sigma_{yy},\ldots,\sigma_{45(zx)}$ are the viscous strain rate and the stress components. Also, we can set the first orthotropic parameter a_1=1 without loss of generality.

A.2 Uniaxial Tests in the X- and Z- Directions

To derive a_2 and a_3, we first obtain expressions for the strain rates in the x- and z-directions using Eqs. (50 - 52) and the definition for the equivalent stress (Eq. 45). Note that the stress vectors are $\underline{\sigma}=[\sigma_{xx}\ 0\ 0\ 0\ 0\ 0]^T$ and $\underline{\sigma}=[0\ 0\ \sigma_{zz}\ 0\ 0\ 0]^T$ for loading in the X- and Z- directions, respectively. Thus:

$$\dot{\varepsilon}_{xx} = a\left(\frac{1+a_3}{1+a_2}\right)^{(N+1)/2} \sigma_{xx}^{N} \tag{A.7}$$

$$\dot{\varepsilon}_{zz} = a\left(\frac{a_2+a_3}{1+a_2}\right)^{(N+1)/2} \sigma_{zz}^{N} \tag{A.8}$$

Equations (A.7) and (A.8) are then compared with Eqs. (A.2) and (A.3), respectively. Solving for a_2 with $\beta_1=(a/b_2)^{1/N}$ in the first pair of equations and with $\beta_2=(a/b_3)^{1/N}$ in the second pair of equations, we obtain two simultaneous equations involving a_2 and a_3:

$$a_2 = (1+a_3)\beta_1^{2N/(N+1)} - 1 \tag{A.9}$$

$$a_2 = (a_2+a_3)\beta_2^{2N/(N+1)} - 1 \tag{A.10}$$

Equations (69) and (70) are obtained by solving Eqs. (A.9) and (A.10) for a_2 and a_3 in terms of β_1 and β_2.

A.3 Uniaxial Tests at 45° on Y-Z , X-Y and Z-X Planes

Consider the case of the uniaxial test at 45° on the y-z plane. The stress applied at 45° to the coordinate axes in the plane is denoted by $\sigma_{45(yz)}$. The corresponding strain is denoted by $\varepsilon_{45(yz)}$. By means of a stress transformation, the plane stress vector $[\sigma_{yy},\sigma_{zz},\sigma_{yz}]^T=[\sigma_{45(yz)}/2,\sigma_{45(yz)}/2,\sigma_{45(yz)}/2]^T$.

After computing the equivalent stress defined in Eq. (45), the inplane strains are computed using Eqs. (50)-(52):

$$\dot{\varepsilon}_{yy} = K\, a_1/6\ \sigma_{45(yz)}^{N} \tag{A.11}$$

$$\dot{\varepsilon}_{zz} = K\, a_3/6\ \sigma_{45(yz)}^{N} \tag{A.12}$$

$$\dot{\gamma}_{yz} = K\, a_5\ \sigma_{45(yz)}^{N} \tag{A.13}$$

where

$$K = a\left(\frac{3}{a_1+a_2}\right)^{(N+1)/2}\left(\frac{a_1+a_3}{3} + 2a_5\right)^{(N-1)/2}(1/2)^{(N-1)} \tag{A.14}$$

The strain rate at 45° to the coordinate axis can be obtained by a strain transformation :

$$\dot{\varepsilon}_{45(yz)} = 1/4 \left(\frac{a_1+a_3}{3} + 2a_5\right) K \sigma_{45(yz)}^{N} \tag{A.15}$$

Comparison of Eqs. (A.4) and (A.15) with $\beta_3=(a/b_4)^{1/N}$ yields an expression for a_5, as given by Eq. (72). To obtain parameters a_4 and a_6, (see Eqs. (71) and (73)) , similar 45° tests can be conducted in the x-y and z-x planes respectively. For a transversely isotropic material, $\beta_2=\beta_3=1$ and $\beta_4=\beta_5$. The constants a_1 to a_5 can then be simplified to the following:

$$a_1 = 1 \tag{A.16}$$
$$a_2 = 2\beta_1^{\,n} - 1 \tag{A.17}$$
$$a_3 = 1 \tag{A.18}$$
$$a_4 = 2\beta_1^{\,n}/6\ (4\beta_4^{\,-n} - 1) \tag{A.19}$$
$$a5 = 2\beta_1^{\,n}/6\ (4 - \beta_1^{\,-n}) \tag{A.20}$$
$$a_6 = 2\beta_1^{\,n}/6\ (4\beta_5^{\,-n} - 1) \tag{A.21}$$

APPENDIX B

Frederking's Tests

B.1 Type A Test

The coordinate axes are defined in the text. The ice sheet is subjected to normal stress σ_{yy} in the y-direction, and its in-plane movement in the z-direction is restrained. Stresses in the x-direction are assumed to be zero. Thus:

$$\sigma_{xx} = 0 \tag{B.1}$$

$$\dot{\varepsilon}_{zz} = 0 \tag{B.2}$$

The derivation below assumes that damage is negligible. Using Eqs. (50)-(52) and (B.2), the following expression is obtained:

$$\sigma_{zz} = \frac{a_2}{a_2+a_3}\sigma_{yy} \tag{B.3}$$

After computing the equivalent stress (Eq. (45)), the strain rate in the y-direction is determined from Eqs. (50)-(52):

$$\dot{\varepsilon}_{yy} = a[\frac{1}{1+a_2}(1 + \frac{a_2 a_3}{a_2+a_3})]^{(N+1)/2} (\sigma_{yy}{}^{c})^N \tag{B.4}$$

where the superscript c on σ_{yy} implies that it is confined. For an unconfined test we have from Eq. (A.1):

$$\dot{\varepsilon}_{yy} = a(\sigma_{yy}{}^{u})^N \tag{B.5}$$

where the superscript u on σ_{yy} implies that it is unconfined. If the strain rates are the same, we can equate Eqs. (B.4) and (B.5) to obtain (with substitutions from Eqs. (A.16)-(A.21) for transverse isotropy) the expression for Γ_z given by Eq. (74).

B.2 Type B Test

The load is applied in the y-direction. Stresses in the z-direction are assumed to be zero. Displacements are constrained in the x-direction. These imply:

$$\sigma_{zz} = 0 \tag{B.6}$$

$$\dot{\varepsilon}_{xx} = 0 \tag{B.7}$$

The same procedure is followed as in the type A test. The equations corresponding to Eqs. (B.3)-(B.4) are, respectively:

$$\sigma_{xx} = \frac{a_1}{a_1+a_3}\sigma_{yy} \tag{B.8}$$

$$\dot{\varepsilon}_{yy} = a[\frac{1}{1+a_2}(a_2 + \frac{a_3}{1+a_3})]^{(N+1)/2} \quad (\sigma_{yy}{}^c)^N \tag{B.9}$$

Comparing Eqs. (B.9) and (B.5), and substituting from Eqs. (A.16)-(A.21), Eq. (75) for Γ_x follows.

APPENDIX C
Triaxial Test

In the triaxial test of a transversely isotropic ice sheet subjected to a normal stress σ in the y-direction, the stress state is described by the vector $[\sigma_{xx}\ \sigma_{yy}\ \sigma_{zz}\ \sigma_{xy}\ \sigma_{yz}\ \sigma_{zx}]^T =$ $[\tau\sigma\ \sigma\ \tau\sigma\ 0\ 0\ 0]^T$, where τ is the ratio of the confining stress to the axial stress. The equivalent stress (Eq. (45)) is $\sigma_e =$ $(1-\tau)\sigma$. The strain rate in the y-direction is obtained from Eqs. (50)-(52) as follows:

$$\dot{\varepsilon}_{yy} = a(1-\tau)^N\,(\sigma_{yy}{}^{tr})^N \tag{C.1}$$

where the superscript 'tr' signifies loading under triaxial conditions. Combining Eqs. (B.5) and (C.1) yields Eq. (76). Also the shear stress normalized by the unconfined stress is independent of τ as shown below:

$$\frac{\sigma_{yy} - \sigma_{zz}}{\sigma_{yy}{}^{u}} = \frac{(1-\tau)\sigma^{yy}{}_{tr}}{\sigma_{yy}{}^{u}} = 1 \tag{C.2}$$

FIGURE CAPTIONS

Figure 1 Dimensionless Strain Rate Plotted Against Dimensionless Time, from the Data of Jacka (1984).

Figure 2 Dimensionless Strain Rate Plotted Against Dimensionless Strain, from the Data of Jacka (1984).

Figure 3 Dimensionless Strain Plotted Against Dimensionless Time, from the Data of Jacka (1984).

Figure 4 Dimensionless Strain Plotted Against Dimensionless Time, from the Data of Sinha (1978).

Figure 5 Strain Dependence of Ratio of Transient Strain to Total Strain for Various Grain Sizes; σ=1.0 MPa at -10°C.

Figure 6 Stress and Strain History and Stress-Strain Results on Columnar-Grained Ice of Average Grain Diameter of 4.5 mm at -10°C for Nominal Strain Rate of 5×10^{-5} s^{-1}.

Figure 7 Comparison Between the Predicted and Experimental Creep and Recovery of Snow Ice. Experimental Data of Brill and Camp Reproduced from Sinha (1979). The Zero Time of Curve (c) is Shifted for Clarity.

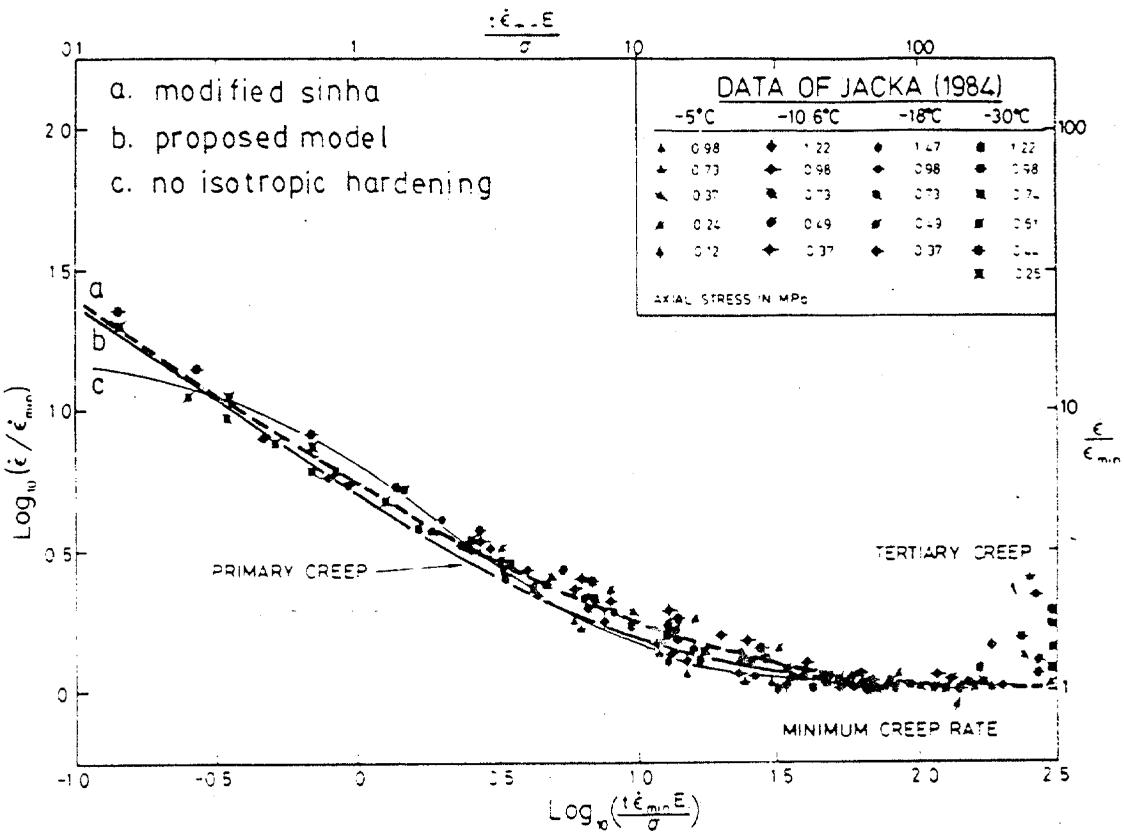

a. modified sinha
b. proposed model
c. no isotropic hardening
DATA OF JACKA (1984)
-5°C
-10.6°C
-18°C
-30°C
AXIAL STRESS IN MPa
PRIMARY CREEP
TERTIARY CREEP
MINIMUM CREEP RATE
$\mathrm{Log}_{10}(\dot{\epsilon}/\dot{\epsilon}_{min})$
$\mathrm{Log}_{10}\left(\frac{t\dot{\epsilon}_{min}E}{\sigma}\right)$
$\frac{\epsilon}{\epsilon_{min}}$

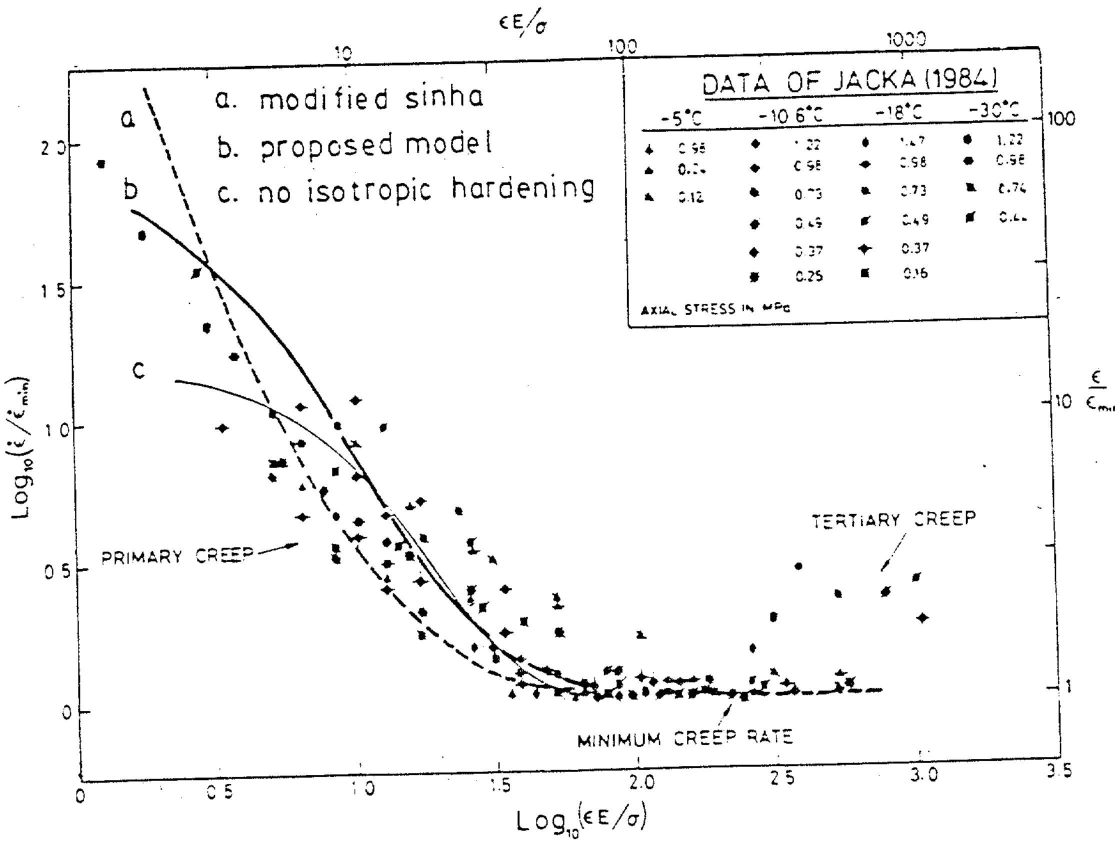

εE/σ
10
100
1000
a. modified sinha
b. proposed model
c. no isotropic hardening
DATA OF JACKA (1984)
-5°C
-10.6°C
-18°C
-30°C
AXIAL STRESS IN MPa
PRIMARY CREEP
TERTIARY CREEP
MINIMUM CREEP RATE
Log10(ε̇/ε̇min)
Log10(εE/σ)

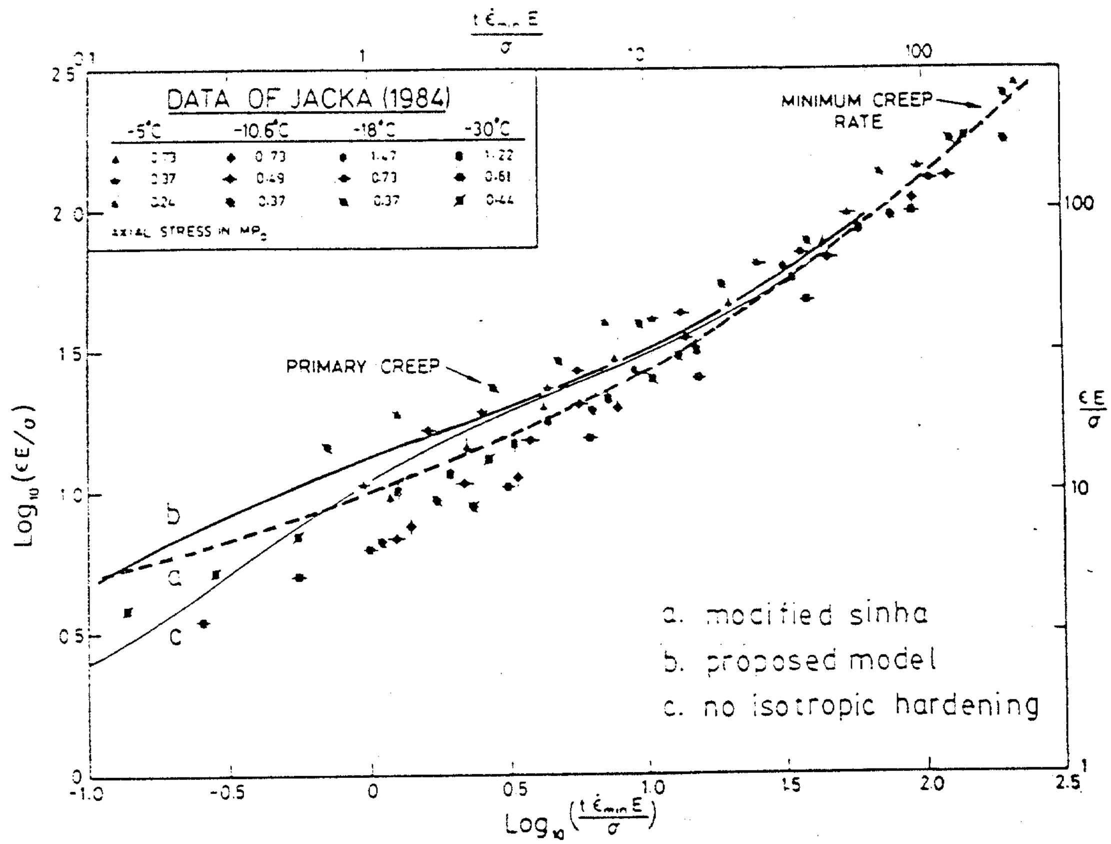

DATA OF JACKA (1984)
-5°C
-10.6°C
-18°C
-30°C
AXIAL STRESS IN MPa
MINIMUM CREEP RATE
PRIMARY CREEP
a. modified sinha
b. proposed model
c. no isotropic hardening
$\mathrm{Log}_{10}(\epsilon E/\sigma)$
$\mathrm{Log}_{10}\left(\frac{t\,\dot{\epsilon}_{min} E}{\sigma}\right)$
$\frac{t\,\dot{\epsilon}_{min} E}{\sigma}$
$\frac{\epsilon E}{\sigma}$

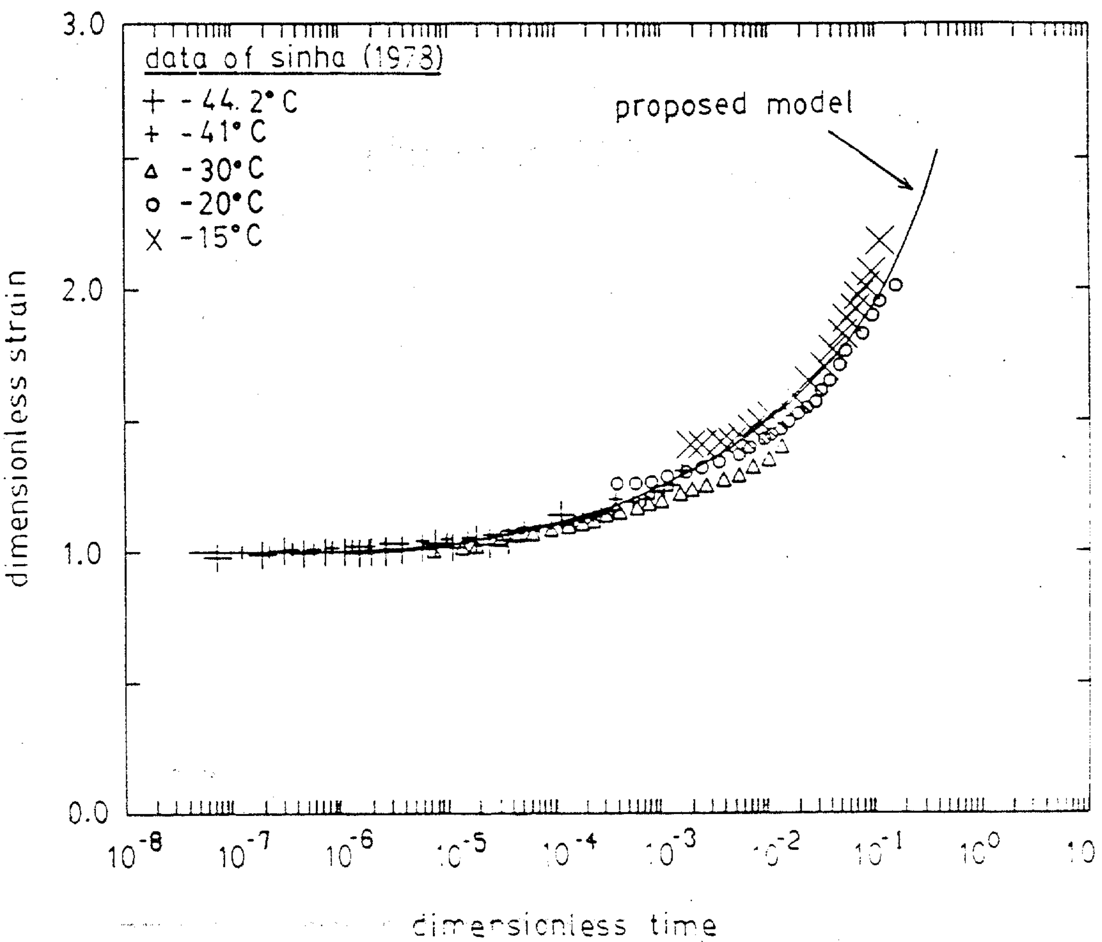
data of sinha (1973)
+ -44.2°C
+ -41°C
△ -30°C
○ -20°C
X -15°C
proposed model
3.0
2.0
1.0
0.0
dimensionless strain
10^-8
10^-7
10^-6
10^-5
10^-4
10^-3
10^-2
10^-1
10^0
10^1
dimensionless time

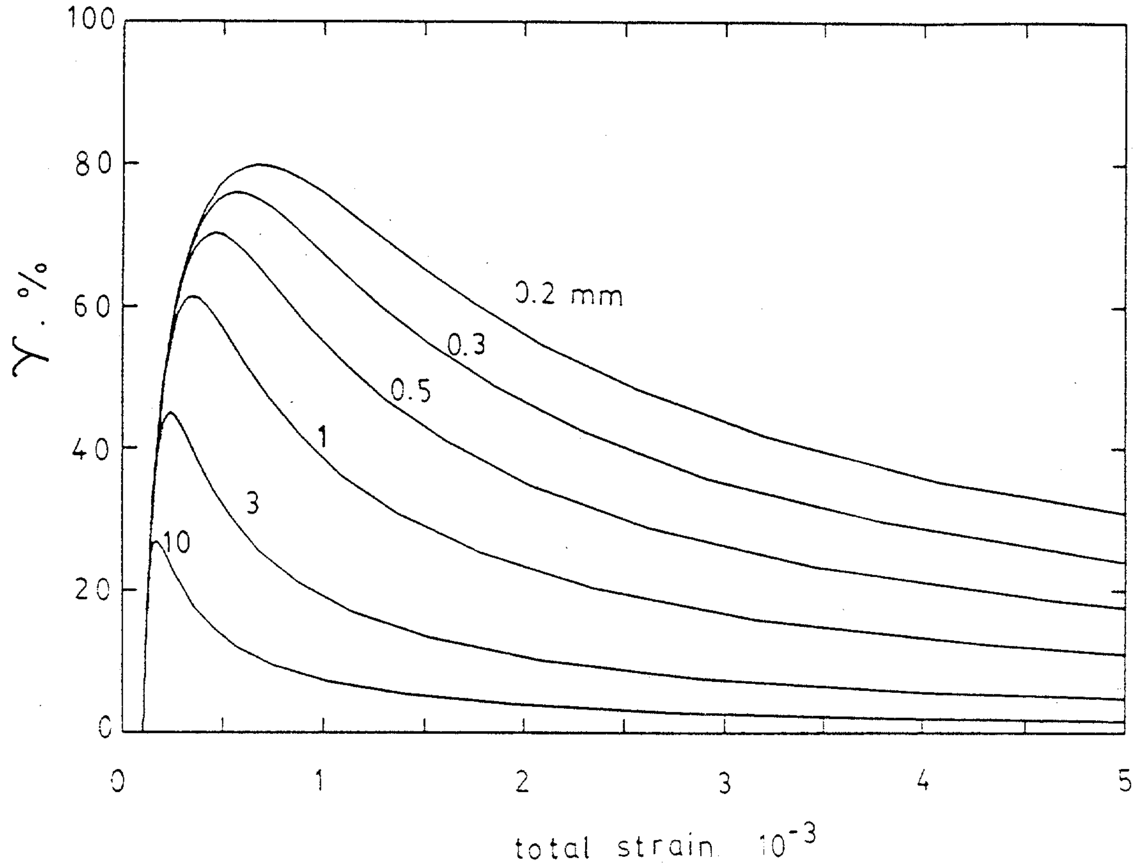
100
80
60
40
20
0
0
1
2
3
4
5
γ . %
total strain 10^-3
0.2 mm
0.3
0.5
1
3
10

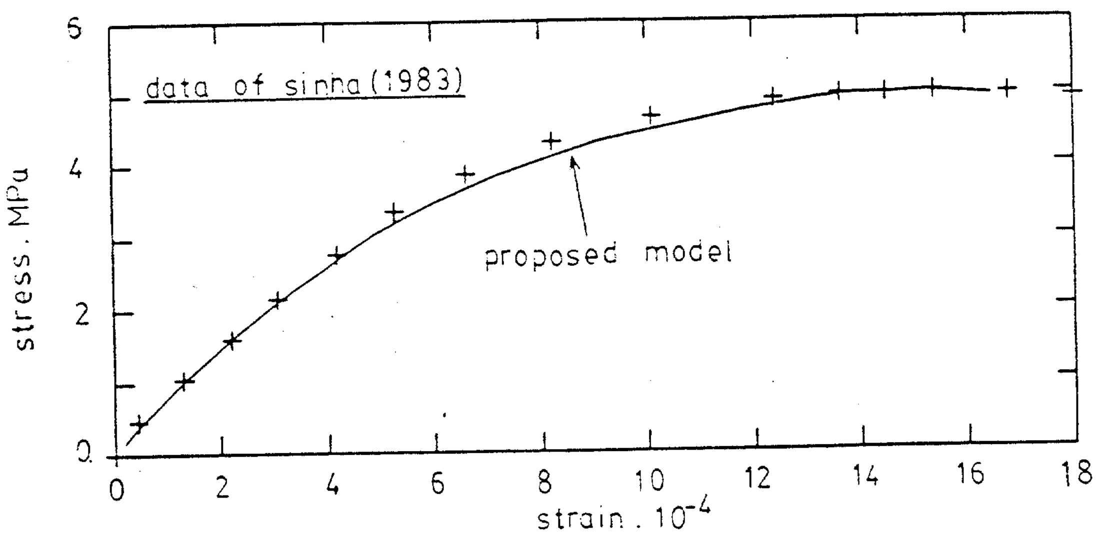
data of sinha (1983)
proposed model
stress . MPa
strain . 10^-4

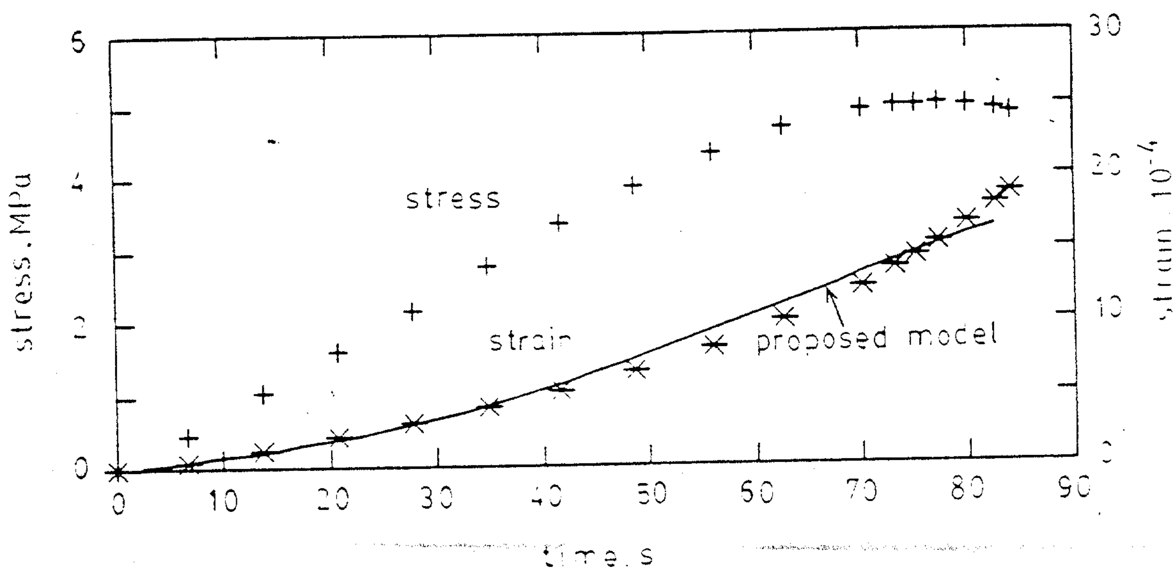
stress
strain
proposed model
stress . MPa
strain 10^-4
time . s

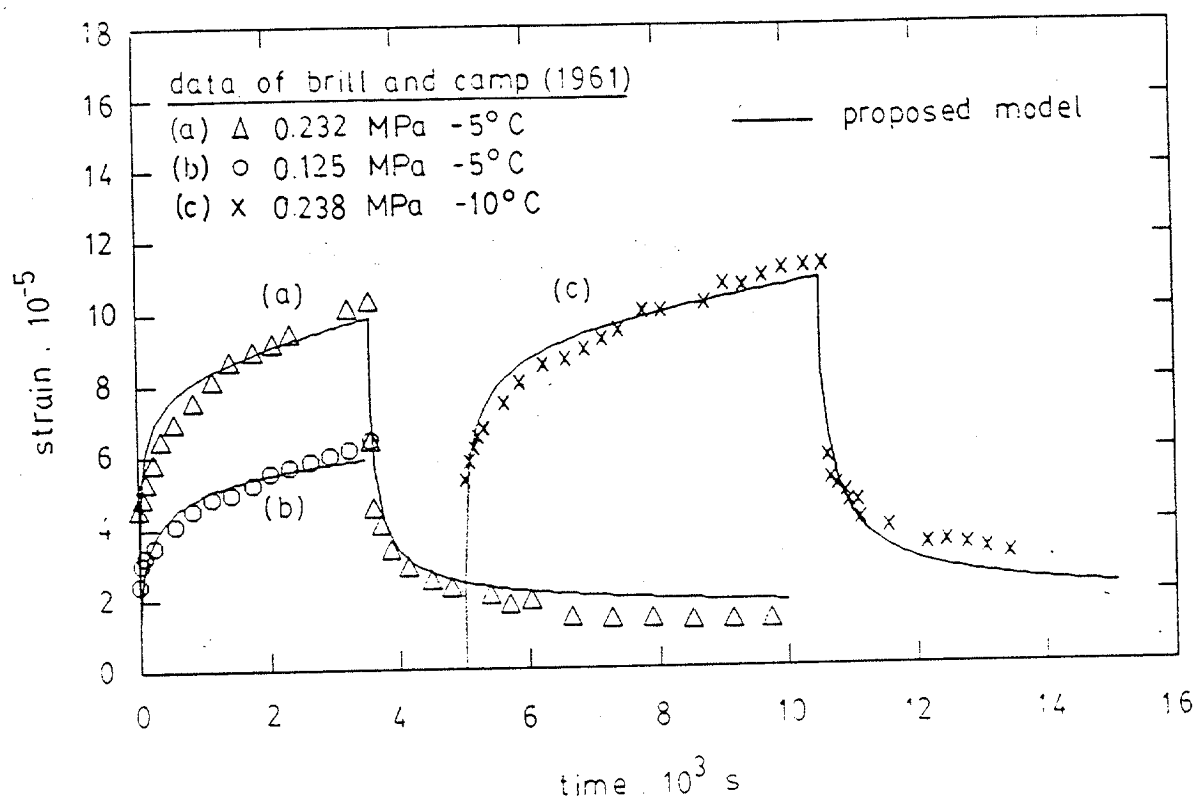

data of brill and camp (1961)
(a) Δ 0.232 MPa -5° C
(b) o 0.125 MPa -5° C
(c) x 0.238 MPa -10° C
proposed model
(a)
(b)
(c)
strain . 10^-5
time . 10^3 s
0
2
4
6
8
10
12
14
16
18